[9] S. O. Kelley, J. K. Barton, N. M. Jackson, L. McPherson, A. Potter, E. M. Spain, M. J. Allen, M. G. Hill, *Langmuir* **1998**, *14*, 6781.
[10] The AFM studies[9] were carried out under electrochemical control, and revealed that the DNA films undergo a potential-dependent change in structure. At open circuit, the monolayer film height is 45(3) Å. Based on the anisotropic dimensions of the 15-base-pair duplexes (20 Å in diameter versus 60 Å in length), this thickness indicates that the helical axis is oriented at about 45° from the gold surface. At applied voltages negative of the potential of zero charge, film thicknesses of about 60 Å are observed; more positive potentials cause a drop in the film height to a limiting value of 20 Å at low surface coverages.
[11] R. Leviky, T. M. Herne, M. J. Tarlov, S. K. Satija, *J. Am. Chem. Soc.* **1998**, *120*, 9787.
[12] F. Arcamone, *Doxorubicin: Anticancer Antibiotics*, Academic Press, New York, **1981**.
[13] a) C. Molinier-Jumel, B. Malfoy, J. A. Reynaud, G. Aubel-Sadron, *Biochem. Biophys. Res. Commun*. **1997**, *84*, 441; b) H. Berg, G. Horn, U. Luthardt, *Bioelectrochem. Bioenerg*. **1981**, *8*, 537.
[14] a) F. Leng, R. Savkur, I. Fokt, T. Przewloka, W. Priebe, J. B. Chaires, *J. Am. Chem. Soc.* **1996**, *118*, 4732; b) A. H.-J. Wang, Y.-G. Gao, Y.-C. Liaw, Y.-K. Li, *Biochemistry* **1991**, *30*, 3812.
[15] A. J. Bard, L. R. Faulkner, *Electrochemical Methods*, Wiley, New York, **1980**.
[16] Based the cross-sectional area of DNA (≈ 3 nm^2) and the geometrical area of the gold electrodes (0.03 cm^2), the maximum surface coverage of DNA is calculated as approximately 6×10^{-11} mol cm^{-2}. The Γ value for DM appears to exceed slightly the theoretical Γ value for DNA, and likely results from electrode surface roughness.
[17] To assess routinely the surface coverage of DM-derivatized DNA on gold, the electrochemical response of $[Fe(CN)_6]^{4-}$ (2 mM) was monitored. This negatively charged ion is repelled from the surface of the modified electrode by the polyanionic DNA, and exhibits essentially no response when the surface is well covered. While not a direct measure of surface coverage, this technique allows the convenient assay of individual electrodes for adequate modification. As the electrode-modification procedure did not always result in uniform surface coverages for the DM-modified duplexes, only electrodes that appeared well covered using both the integrated current of the DM reduction and the ferrocyanide test were studied.
[18] Based on molecular modeling, if DM is bound at the end of the duplex closest to the electrode (Figure 3a), the through-helix DM – electrode separation is greater than 10 Å; if the intercalator is cross-linked to the end of the duplex farthest from the electrode, the DM-electrode separation is greater than 35 Å (Figure 3b).
[19] R. A. Marcus, N. Sutin, *Biochim. Biophys. Acta* **1985**, *811*, 265.
[20] For discussions of some possible mechanisms, see a) A. K. Felts, W. T. Pollard, R. A. Freisner, *J. Phys. Chem*. **1995**, *99*, 2929; b) S. Priyadarshy, S. M. Risser, D. N. Beratan, *J. Biol. Inorg. Chem.* **1998**, *3*, 196; c) J. Jortner, M. Bixon, T. Langenbacher, M. E. Michel-Beyerle, *Proc. Natl. Acad. Sci. USA* **1998**, *95*, 12759; d) A. Okada, V. Chernyak, S. Mukamel, *J. Phys. Chem*. **1998**, *102*, 1241; e) E. S. Chen, E. C. M. Chen, *Bioelect. Bioenerg*. **1998**, *46*, 15.
[21] See, for example, Z. Q. Feng, S. Imabayashi, T. Kakiuchi, K. Niki, *J. Electroanal. Chem*. **1996**, *408*, 15.
[22] a) D. J. Patel, S. A. Kozlowski, S. Ikuta, K. Itakura, *FASEB J.* **1984**, *11*, 2664; b) F. Aboul-ela, D. Koh, I. Tinoco, F. H. Martin, *Nucleic Acids Res.* **1985**, *13*, 4811.
[23] T. Ihara, J. Takata, H. Takagi, *Anal. Chim. Acta* **1998**, *365*, 49.
[24] The coulometry of DM at electrodes modified with CA-containing duplexes varied to some degree as a function of the surface coverage. At high surface coverages (as determined by the ferrocyanide assay), essentially no signal was observed with the mismatched duplexes. However, at more moderate surface coverages, small signals corresponding to the reduction of DM were found. These typically did not exceed 30% of the signals found for the TA duplexes. The morphology of partial DNA monolayers is unknown.
[25] The AFM measurements revealed monolayer thicknesses of about 40 Å at open circuit for both CA- and TA-containing duplexes; moreover, the oxidation of ferrocyanide was similarly attenuated at both surfaces. Expected masses for DM-cross-linked DNA duplexes (accounting for the one-base change) were measured by mass spectrometry, and spectrophotometric assays revealed that the extent of cross-linking was identical in both fully paired and mismatched sequences.
[26] a) K. M. Millan, S. R. Mikkelsen, *Anal. Chem*. **1993**, *65*, 2317; b) K. Hashimoto, K. Ito, Y. Ishimori, *Anal. Chem*. **1994**, *66*, 3830; c) X.-H. Xu, A. J. Bard, *J. Am. Chem. Soc.* **1995**, *117*, 2627; d) J. Wang, X. Cai, G. Rivas, H. Shiraishi, P. A. M. Farias, N. Dontha, *Anal. Chem*. **1996**, *68*, 2629.
[27] S. O. Kelley, E. M. Boon, J. K. Barton, N. M. Jackson, M. G. Hill, *Chem. Biol.*, submitted.
[28] a) S. Priyadarshy, S. M. Risser, D. N. Beratan, *J. Phys. Chem*. **1996**, *100*, 17678; b) J. M. Warman, M. P. de Haas, A. Rupprecht, *Chem. Phys. Lett*. **1996**, *249*, 319; c) D. N. Beratan, S. Priyadarshy, S. M. Risser, *Chem. Biol.* **1997**, *4*, 3; d) T. L. Netzel, *J. Chem. Educ*. **1997**, *74*, 646; e) E. S. Krider, T. J. Meade, *J. Biol. Chem*. **1998**, *3*, 222.
[29] Y. Okahata, T. Kobayashi, K. Tanaka, M. Shimomura, *J. Am. Chem. Soc.* **1998**, *120*, 6165.
[30] L. Wachter, J. A. Jablonski, K. L. Ramachandran, *Nucleic Acids Res.* **1986**, *14*, 7985.
[31] J. G. Harrison, S. Balasubramanian, *Bioorg. Med. Chem. Lett*. **1997**, *7*, 1041.
[32] P. W. Riddles, R. L. Blakeley, B. Zerner, *Anal. Biochem*. **1979**, *94*, 75.
[33] For example, the oligonucleotide SH-(CH_2)CONH$(CH_2)_6$NHCO$_2$-$^{5'}$ATCCTACTCATGGAC hybridized with the inosine complement was modified with DM and analyzed by MALDI-TOF spectrometry. Mass-to-charge ratios of 5284 (calcd: 5282; DM + SH strand), 4541 (calcd: 4540; (complement), and 4742 (calcd: 4742; SH strand) were detected. These values correspond to the calculated masses for fragments expected from this duplex. UV/Vis absorption spectroscopy also revealed a duplex:DM stoichiometry of 1:1 based upon comparison of the duplex absorbance at 260 nm and the absorbance of intercalated DM at 480 nm ($\varepsilon = 7.5 \times 10^3$ M^{-1} cm^{-1}). In the presence of 100 mM phosphate and 100 mM $MgCl_2$ (pH 7), thermal denaturation studies of 5 μM duplexes (monitored by absorbance at 260 nm) revealed melting temperatures of 48 and 50 °C for the native and DM-cross-linked duplexes, respectively. A similar melting profile was obtained by monitoring hypochromicity at 482 nm for the DM duplex.
[34] L. Tender, M. T. Carter, R. W. Murray, *Anal. Chem*. **1994**, *66*, 3173.

Electron Tunneling in DNA**

Anthony Harriman*

The idea that DNA is an effective medium for long-range electron tunneling is far from new.[1] Radiation biologists invoked this concept almost 40 years ago to account for the unusually high conductivity of solid DNA.[2] Later studies found that the conductivity arose from ice particles.[3] The effect has also been explained in terms of high charge mobility along the outside of the duplex.[4] Both EPR[5] and luminescence[6] results have been interpreted in terms of long-range electron tunneling whereas pulse radiolysis studies[7] indicate electron tunneling is restricted to less than five base pairs. Other investigators searched in vain for soliton effects.[8] More

[*] Prof. A. Harriman
Laboratoire de Chimie, d'Electronique et Photonique Moléculaires
Ecole Européenne de Chimie, Polymères et Matériaux (ECPM)
Université Louis Pasteur
25, rue Becquerel, F-67087 Strasbourg Cedex (France)
Fax: (+33) 494-99-92-56
E-mail: harriman@chimie.u-strasbg.fr

[**] This work was supported by the Royal Society of London.

recently, Barton and colleagues[9–13] have reported several examples of long-range electron tunneling between intercalated reagents separated by up to 40 Å and proposed that the rate of electron transfer shows a remarkably weak dependence on the number of interspersed base pairs. These conclusions are inconsistent with all other experimental observations concerning electron transfer in DNA.[14–21] Furthermore, X-ray structural data[22] indicate that repair photoenzymes operate over short distances and there is no obvious biological function that requires DNA to be an effective conduit for long-range electron tunnelling.

The number of experiments that address electron transfer in DNA remains limited, however, while theoretical evaluations[23–25] appear contradictory. Unlike proteins,[23] little is known about the ability of the DNA duplex to support electron transfer and, in particular, the size of the reorganization energy (λ) that accompanies electron transfer is unknown. This latter parameter, being crucial for an improved theoretical understanding of long-range electron tunneling, is a key feature of nonadiabatic electron-transfer reactions[26] and ranges from about 0 eV in a frozen glass to almost 2 eV in polar solvents.[27] It becomes of special significance when the thermodynamic driving force for electron transfer (ΔG^0) is small, since it is the interplay between λ and ΔG^0 that determines the activation energy for the electron-transfer event.[26] Herein we measure λ values for both interfacial and through-strand electron transfer and show that the derived value is similar to that found for protein matrices.[28]

Electron tunneling in DNA can be categorized according to the mutual positioning of the redox partners. The simplest case concerns interfacial electron transfer from an intercalated dye molecule to a positively-charged electron acceptor bound to the external phosphate chain. An appropriate redox pair, first studied by Fromherz and Rieger,[29] comprises intercalated ethidium bromide (EB^+) as the donor and *N*,*N*′-dimethyl-4,4′-bipyridinium dichloride (MV^{2+}) as the surface-bound acceptor. Electron transfer from the singlet excited state of intercalated EB^+ to MV^{2+} ($\Delta G^0 \approx -0.08$ eV) can be monitored by steady-state and time-resolved fluorescence spectroscopy.[15] The quenching of EB^+ fluorescence increases progressively with increasing concentration of MV^{2+} until the phosphate chain is saturated with bound MV^{2+}. Beyond this point, further increases in MV^{2+} concentration have no effect (Figure 1 A). At saturation, the position of MV^{2+} is frozen on the time scale of electron transfer, with the shortest edge-to-edge separation distance ($R \approx 4$ Å) being set by the occupancy number of each reagent. Under these conditions the rate constant for interfacial electron transfer between nearest neighbors at 20 °C ($k_{ET} = 6.3 \times 10^8\ s^{-1}$) can be determined according to Equation (1) from fluorescence lifetimes measured in the presence ($\tau_F = 1.5$ ns) and absence ($\tau_F^0 = 25.5$ ns) of MV^{2+} (Figure 1 B) The derived rate constant was found to be

$$k_{ET} = \frac{1}{\tau_F} - \frac{1}{\tau_F^0} \quad (1)$$

independent of ionic strength, type of background electrolyte, and concentration of MV^{2+} provided saturation prevailed, but was markedly dependent on temperature over the range $8 < T < 50$ °C. In fact, k_{ET} increases smoothly with increasing

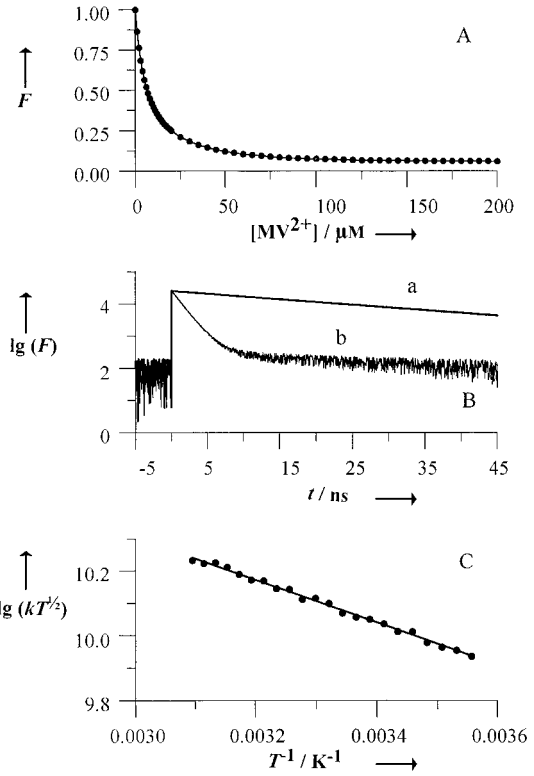

Figure 1. A) Effect of added MV^{2+} on the relative fluorescence yield *F* for EB^+ (4 μM) intercalated into calf-thymus DNA (100 μM). The solid line drawn through the data points corresponds to a binding constant of $1 \times 10^5\ M^{-1}$ for association of MV^{2+} to the exterior of the duplex; the ratio of initial and saturation *F* values is 16. B) Fluorescence decay profiles for EB^+ (4 μM) intercalated into DNA (100 μM) a) in the absence of MV^{2+} and b) at saturation. C) Effect of temperature on the rate constant for electron transfer from intercalated EB^+ to surface-bound MV^{2+} expressed in the form of Equation (2).

temperature (Figure 1 C) as expected for activated nonadiabatic electron transfer.[26] This allows calculation of the free energy change of activation ($\Delta G^{\neq}$) from Equation (2) as being 0.129 ± 0.005 eV and giving a pre-exponential factor *A* of $(1.84 \pm 0.05) \times 10^{12}\ s^{-1} K^{1/2}$.

$$k_{ET}\sqrt{T} = A \exp\left(-\frac{\Delta G^{\neq}}{k_B T}\right) \quad (2)$$

Marcus theory[26] expresses $\Delta G^{\neq}$ in terms of the thermodynamic driving force (ΔG^0) and the total reorganization energy (λ) that accompanies interfacial electron transfer [Eq. (3)]. Thus, the reorganization energy is approximately

$$\Delta G^{\neq} = \frac{(\lambda + \Delta G^0)^2}{4\lambda} \quad (3)$$

0.66 eV, which is much closer to that of a protein ($\lambda \approx 0.4$ eV[28]) than a polar solvent ($\lambda \approx 1.5$ eV).[27] This result suggests that the duplex both screens the acceptor from solvent effects and minimizes structural distortion during electron transfer. Replacing EB^+ with acridine orange ($\lambda = 0.70$ eV), palladium tetrakis(*N*-methyl-4-pyridinium)porphyrin ($\lambda = 0.67$ eV), or 9-methylacridinium cations ($\lambda = 0.68$ eV) results in an average λ value of 0.68 ± 0.04 eV. Furthermore,

 © WILEY-VCH Verlag GmbH, D-69451 Weinheim, 1999 1433-7851/99/3807-0946 $ 17.50+.50/0 *Angew. Chem. Int. Ed.* **1999**, *38*, No. 7

evaluation of the pre-exponential factor according to Equation (4)[26] shows that the electronic coupling matrix element

$$A = \frac{2\pi V^2}{\hbar\sqrt{4\pi\lambda k_B}} \quad (4)$$

V for the EB^+/MV^{2+} system has a value of approximately $18\,cm^{-1}$. This latter value indicates weak coupling occurs between the closely spaced reactants, which gives rise to an activationless rate constant of about $1 \times 10^{11}\,s^{-1}$ at 20 °C, and confirms the validity of Marcus theory to this system.

A second case concerns electron transfer between intercalated reagents separated by several base pairs.[14] To ensure consistency of the interspersed medium DNA was replaced with the synthetic polynucleotides poly[dGdC]·poly[dGdC] (poly[dGdC]) and poly[dAdT]·poly[dAdT] (poly[dAdT]) while MV^{2+} was replaced by *N*,*N*′-dimethyl-2,9-diazapyrenium dichloride (DAP^{2+}). This latter acceptor intercalates avidly but randomly into the polynucleotide[30] relative to an incumbent EB^+ molecule. The closest approach between these reactants, which is set by the mutual exclusion principle, corresponds to three interspersed base pairs such that, assuming a regular duplex, the miminum edge-to-edge separation will be 10.2 Å. Larger separations abound but these will be quantized since there must be a whole number of interspersed base pairs. This latter realization is the key element in our experimental attempt to measure the electronic conductivity of DNA by high-resolution, time-resolved fluorescence spectroscopy. Thus, if the duplex provides an extremely effective pathway for electron transfer between intercalated reagents the fluorescence lifetime of EB^+ will show only a shallow dependence on the separation distance and the decay profile will appear as a distribution of similar decay rates. Detailed analysis of such profiles can be made only if the shape of the distribution function is known. However, in the event that the duplex is a poor electronic conductor the fluorescence lifetime of intercalated EB^+ will depend strongly on the separation distance and, since only certain separations are possible, the decay profile will appear as a series of exponential functions. In this case individual lifetimes extracted from computer fitting of the decay data can be attributed to pairs of reactants separated by discrete distances, each being a multiple of 3.4 Å, so that the difference between lifetimes provides a direct measure of the damping effect of the duplex.

In all our experiments the fluorescence decay profiles recorded in the presence of intercalated DAP^{2+} correspond to the sum of three exponential components, compared to the single-exponential decay observed in the absence of DAP^{2+} (Figure 2 A). The derived lifetimes remain independent of the amount of DAP^{2+} loaded onto the strand, but the contribution of the shortest lifetime increases as more DAP^{2+} is bound. Laser flash photolysis studies have confirmed that fluorescence quenching is a consequence of electron transfer to the intercalated acceptor. Equation (1) then allows three k_{ET} values to be derived for each concentration of DAP^{2+}. Each rate constant can be assigned to electron transfer across a given number of interspersed base pairs, with the rate decreasing as the reactants become more remote. These

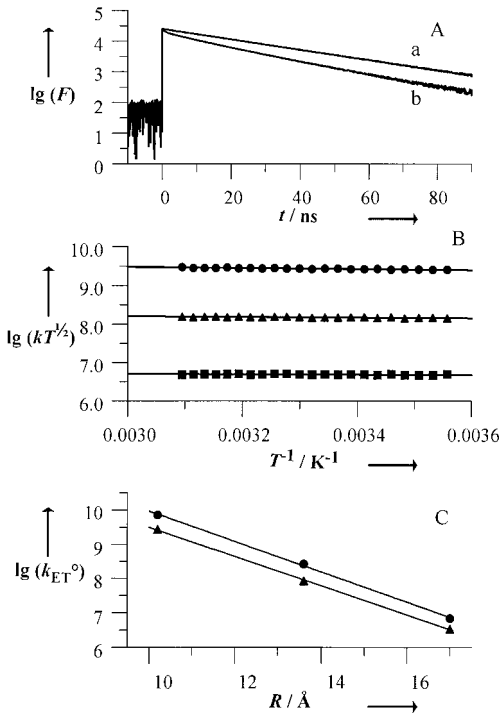

Figure 2. A) Fluorescence decay profiles for EB^+ (4 μM) intercalated into poly[dAdT] (100 μM) a) in the absence of an electron acceptor and b) in the presence of intercalated DAP^{2+} (10 μM). B) Effect of temperature on the rate constant for electron transfer from EB^+ (4 μM) to DAP^{2+} (15 μM) when both are intercalated into poly[dAdT] as measured over separation distances of 10.2 (●), 13.6 (▲), and 17.0 Å (■). C) Relationship between the activationless rate constant for electron transfer from intercalated EB^+ to intercalated DAP^{2+} and the separation distance (R). Data refer to poly[dAdT] (●) and poly[dGdC] (▲) at 20 °C. The solid lines correspond to fits to Equation (5) with $\beta = 1.0\ Å^{-1}$.

derived k_{ET} values, therefore, must be associated with reactant pairs separated by three, four, or five base pairs.[14] At larger separations the fluorescence lifetime remains unquenched because light-induced electron transfer cannot compete with the inherent deactivation processes when the reactants are separated by more than six base pairs.

This strategy allows rates of through-strand electron tunneling to be derived for the three shortest separation distances R of 10.2, 13.6, and 17.0 Å. The rates found at 20 °C decrease markedly with increasing separation over the limited range available, and it is immediately made clear that DNA is a relatively poor conduit for electrons. More surprisingly is the observation that the rate is quite sensitive to the composition of the duplex (Table 1). The rate of electron tunneling is faster for poly[dAdT] than for poly[dGdC] at each separation distance. These rates are weakly dependent on temperature (Figure 2 B), such that Equations (1) – (4) allow calculation of λ and V values for the two polynucleotides (Table 1).

It is notable that $\Delta G^{\neq}$ decreases with increasing separation and, assuming the constancy of ΔG^0 ($= -0.26$ eV), this must be a consequence of changes in the λ values. This latter effect is most likely caused by slight distortion of the double helix at short separations[31] and, as the duplex becomes more regular, λ approaches a value of approximately 0.4 eV. Thus, the

 © WILEY-VCH Verlag GmbH, D-69451 Weinheim, 1999 1433-7851/99/3807-0947 $ 17.50+.50/0

Table 1. Parameters derived for through-strand electron tunneling involving intercalated reagents at 20 °C. Experimental conditions are as described in the legend to Figure 2.

R [Å][a]	k_{ET} [s^{-1}][b]	$\Delta G^{\neq}$ [eV][c]	λ [eV][d]	V [cm^{-1}][e]	k^0_{ET} [s^{-1}][f]
		poly[dAdT]			
10.2	2.7×10^9	0.025	0.48	4.4	7.2×10^9
13.6	1.5×10^8	0.015	0.42	0.82	2.7×10^8
17.0	4.8×10^6	0.0095	0.38	0.13	7.0×10^6
		poly[dGdC]			
10.2	1.1×10^9	0.023	0.47	2.7	2.7×10^9
13.6	4.3×10^7	0.018	0.44	0.47	8.6×10^7
17.0	2.0×10^6	0.014	0.41	0.09	3.4×10^6

[a] Edge-to-edge distance separating the intercalated reagents calculated from the binding isotherms and assuming the validity of the mutual exclusion principle. [b] Rate constant for electron transfer at 20 °C measured by time-resolved fluorescence spectroscopy, ±10%. [c] Activation free-energy change for through-strand electron tunneling derived from Equation (2), ±10%. [d] Total reorganization energy accompanying electron transfer as calculated from Equation (3), ±10%. [e] Electronic coupling matrix element as calculated from Equation (4), ±15%. [f] Activationless rate constant for electron transfer, ±15%.

reorganization energy is remarkably similar to that found for proteins and is much smaller than normally observed for electron transfer in polar solvents. A small λ value, a natural consequence of a rigid matrix that is not readily polarized, favors rapid electron tunneling at modest thermodynamic driving forces, since such reactions will take place close to the apex of a Marcus rate versus energy-gap profile, and lowers the activation energy. In this respect, we might anticipate fast rates of both through-strand and interfacial electron transfer for DNA-bound reagents.

The derived activationless rate constants k^0_{ET}, these being corrected for variations in both λ and $\Delta G^{\neq}$, can be used to refine earlier estimates of how the duplex attenuates electron tunneling.[14, 32] Thus, the distance dependence for the rate of electron transfer can be expressed in terms of Equation (5)[26] where β is an attenuation coefficient that quantifies the

$$k^0_{ET} = k^0 \exp^{-\beta R} \quad (5)$$

damping effect of the interspersed medium. From the k^0_{ET} values derived for each polynucleotide at discrete separation distances (Table 1), we obtain $\beta = 1.00 \pm 0.06$ Å^{-1}, regardless of the composition of the strand. Again, this β value lies close to that reported for protein matrices[23] and is inconsistent with fast long-range electron transfer. That the rate shows an exponential dependence on separation distance (Figure 2C) in both cases is indicative of poor connectivity between stacked base pairs and not because of restricted coupling between intercalated reagent and adjacent nucleotide.

Our analysis shows that poly[dAdT] provides better electronic coupling than does poly[dGdC]. This can be seen by comparing the rates at any fixed distance (Table 1) and is also apparent from the derived rate constants for electron tunneling at orbital contact (k^0). The inherent rate for poly[dAdT] is some fourfold faster than that for poly[dGdC] ($k^0 = 2.5 \times 10^{14}$ s^{-1} and $k^0 = 5.8 \times 10^{13}$ s^{-1}, respectively). Given that β is identical for both polynucleotides, the enhanced rate must arise from an improved blending of LUMOs localized on the reactants and adjacent nucleotides, either with respect to relative energy levels or coupling coefficients, if electron tunneling occurs by way of superexchange interactions.[33] The derived k^0 values are very high, but are offset by the protein-like β value, which causes V to decreases rapidly with increasing separation.

The examination of the ability of polynucleotides to conduct electrons over quite short (<20 Å) distances in this study has revealed two antagonistic aspects of the duplex. The inherent rigidity and restricted solvation combine to lower the total reorganization energy that accompanies electron transfer and this facilitates fast electron tunneling, even at low temperature and with minimal thermodynamic driving force. This is restricted to short-range interactions, however, by weak electronic coupling between reactants, regardless of whether electron transfer is through-strand or interfacial. In the former case the problem arises from poor connectivity between stacked base pairs and is not associated with the choice of reactants. Restricted orbital overlap is responsible for the limited electronic communication when the reactants are separated by an interface and, in this case, the non-intercalated reagent must migrate along the phosphate backbone until it reaches the optimum site for electron transfer. The net conclusion is that DNA is a highly appropriate medium for fast, but close-range electron tunneling and this provides the rationale for the manner in which repair photoenzymes operate.[22, 34] The poor connectivity between stacked base pairs can be considered as a protective measure to inhibit long-range electron tunneling and to restrict all such reactions to short-range events.

Experimental Section

Materials were obtained from Sigma Chemicals or were available from earlier investigations. Solutions of the polynucleotides were prepared in freshly-distilled water containing 5 mM phosphate buffer (pH 7) and 5 mM sodium sulfate and concentrations, expressed on the basis of nucleotide phosphate, were determined by absorption spectroscopy.[14, 15] An aliquot of the intercalator, prepared in the same medium, was injected into the polynucleotide solution and equilibrated for 1 h. The final concentration was measured by absorption spectroscopy. A titration was made by adding aliquots of standard solutions of MV^{2+} or DAP^{2+} and the course of the reaction was followed by steady-state fluorescence spectroscopy. The temperature was controlled to within 0.1 °C by a circulating pump. Fluorescence lifetimes were measured by time-correlated, single-photon counting methodology using an Antares 76S Nd-YAG laser to pump a Rhodamine 6G or Styryl-9 dye laser that allowed selective excitation of intercalated dye. The temporal resolution of this instrument, after deconvolution of the laser pulse, was approximately 20 ps. See references [14, 15] for more details.

Received: October 16, 1998 [Z 12534 IE]
German version: *Angew. Chem.* **1999**, *111*, 996 – 1000

Keywords: bioorganic chemistry · DNA repair · electron transfer · fluorescence spectroscopy · supramolecular chemistry

[1] B. B. Singh, *Adv. Med. Phys.* **1968**, *12*, 245.
[2] D. D. Eley, D. I. Spivey, *Trans. Faraday Soc.* **1962**, *58*, 411.
[3] D. van Lith, J. M. Warman, M. P. de Haas, A. Hummel, L. Prinsen, *J. Chem. Soc. Faraday Trans.* **1986**, *82*, 2933, 2945.
[4] J. M. Warman, M. P. de Haas, A. Rupprecht, *Chem. Phys. Lett.* **1996**, *249*, 319.

 © WILEY-VCH Verlag GmbH, D-69451 Weinheim, 1999 1433-7851/99/3807-0948 $ 17.50+.50/0

[5] S. Gregoli, M. Olast, A. Bertinochamps, *Radiat. Res.* **1982**, *89*, 238.
[6] E. M. Fielden, S. L. Lillicrap, A. B. Robins, *Radiat. Res.* **1971**, *48*, 421.
[7] D. W. Whillans, *Biochim. Biophys. Acta* **1975**, *414*, 193.
[8] a) K. F. Baverstock, R. B. Cundall, *Radiat. Phys. Chem.* **1988**, *32*, 553; b) M. Cullis, J. D. McClymont, M. C. R. Symons, *J. Chem. Soc. Faraday Trans.* **1990**, *86*, 591.
[9] C. J. Murphy, M. R. Arkin, Y. Jenkins, N. D. Ghatlia, S. H. Bossmann, N. J. Turro, J. K. Barton, *Science* **1993**, *262*, 1025.
[10] M. R. Arkin, E. D. A. Stemp, R. E. Holmlin, J. K. Barton, A. Hörmann, E. J. C. Olson, P. F. Barbara, *Science* **1996**, *273*, 475.
[11] R. E. Holmlin, E. D. A. Stemp, J. K. Barton, *J. Am. Chem. Soc.* **1996**, *118*, 5236.
[12] S. O. Kelley, R. E. Holmlin, E. D. A. Stemp, J. K. Barton, *J. Am. Chem. Soc.* **1997**, *119*, 9861.
[13] S. O. Kelley, J. K. Barton, *Chem. Biol.* **1998**, *5*, 413.
[14] A. M. Brun, A. Harriman, *J. Am. Chem. Soc.* **1992**, *114*, 3656.
[15] A. M. Brun, A. Harriman, *J. Am. Chem. Soc.* **1994**, *116*, 10383.
[16] T. J. Meade, J. F. Kayyem, *Angew. Chem.* **1995**, *107*, 358; *Angew. Chem. Int. Ed. Engl.* **1995**, *34*, 352.
[17] S. J. Atherton, P. C. Beaumont, *J. Phys. Chem.* **1995**, *99*, 12025.
[18] P. Lincoln, E. Tuite, B. Nordén, *J. Am. Chem. Soc.* **1997**, *119*, 1454.
[19] F. D. Lewis, T. Wa, Y. Zhang, R. L. Letsinger, S. R. Greenfield, M. R. Wasielewski, *Science* **1997**, *277*, 673.
[20] K. Fukui, K. Tanaka, *Angew. Chem.* **1998**, *110*, 162; *Angew. Chem. Int. Ed.* **1998**, *37*, 158.
[21] E. Meggers, D. Kusch, M. Spichty, U. Wille, B. Giese, *Angew. Chem.* **1998**, *110*, 465; *Angew. Chem. Int. Ed.* **1998**, *37*, 460.
[22] a) H.-W. Park, S.-T. Kim, A. Sancar, J. Deisenhofer, *Science* **1995**, *268*, 1866; b) T. Tamada, K. Kitadokoro, Y. Higuchi, K. Inaka, A. Yasui, P. E. de Ruiter, A. P. M. Eker, K. Miki, *Nature Struct. Biol.* **1997**, *11*, 887.
[23] a) S. Priyadarshy, D. N. Beratan, S. M. Risser, *Int. J. Quantum Chem.* **1996**, *60*, 1789; b) S. Priyadarshy, S. M. Risser, D. N. Beratan, *J. Phys. Chem.* **1996**, *100*, 17678; c) D. N. Beratan, S. Priyadarshy, S. M. Risser, *Chem. Biol.* **1997**, *4*, 3.
[24] A. K. Felts, W. T. Pollard, R. A. Freisner, *J. Phys. Chem.* **1995**, *99*, 2929.
[25] S. K. Mukamel, *J. Phys. Chem. A* **1998**, *102*, 1241.
[26] R. A. Marcus, N. Sutin, *Biochim. Biophys. Acta* **1985**, *811*, 265.
[27] A. Harriman, V. Heitz, M. Ebersole, H. van Willigen, *J. Phys. Chem.* **1994**, *98*, 4982.
[28] L. G. Arnaut, S. J. Formosinho, *J. Photochem. Photobiol. A* **1997**, *111*, 111.
[29] P. Fromherz, B. Rieger, *J. Am. Chem. Soc.* **1986**, *108*, 5361.
[30] A. M. Brun, A. Harriman, *J. Am. Chem. Soc.* **1991**, *113*, 8154.
[31] The increased λ value found at shorter separations suggests that the reactants are more exposed to solvent molecules and reside in a less rigid environment.
[32] The literature includes several reports of β values (given in units of $Å^{-1}$) for electron tunneling in DNA or short synthetic duplexes: $\beta =$ 0.88[14], 0.73[17], 0.64[19], 1.42[20], 1.00[21], < 0.2[9], < 0.2[10]. A value of $\beta =$ 1.9 $Å^{-1}$ has been given for light-induced electron exchange (that is, simultaneous two-site electron and hole transfer).[15]
[33] S. M. Risser, D. N. Beratan, T. J. Meade, *J. Am. Chem. Soc.* **1993**, *115*, 2508.
[34] a) J. E. Hearst, *Science* **1995**, *268*, 1858; b) A. Sancar, *Biochemistry* **1994**, *33*, 2.

Inter- or Intramolecular Carbometalation of Nonactivated Alkynes by Zirconacyclopentanes in the Presence of Copper Chloride**

Yuanhong Liu, Baojian Shen, Martin Kotora, and Tamotsu Takahashi*

Addition of metal–carbon bonds to alkynes is an attractive methodology for the construction of complex molecules.[1, 2] This approach has been successfully applied to the formation of stereo-defined alkene derivatives. Alkylzirconocene derivatives have been useful in organic synthesis because they are easily prepared by hydrozirconation of alkenes,[3] by alkylation of $[Cp_2ZrCl_2]$ ($Cp = C_5H_5$), or by olefin coupling on zirconocenes.[4] Carbometalation of nonactivated alkynes with alkylzirconocenes would be a useful synthetic tool. However, to the best of our knowledge, no such reactions have been reported. Here we would like to fill this void and present a novel procedure for the direct conversion of zirconacyclopentanes into six- and five-membered ring carbocycles by means of inter- and intramolecular carbometalation of nonactivated alkynes (Scheme 1).

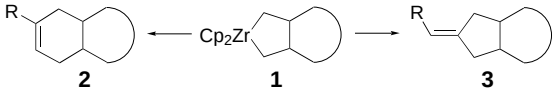

Scheme 1. Conversion of zirconacycles **1** into five- and six-membered ring carbocycles.

Initially, we investigated the carbometalation[5] of nonactivated terminal alkynes with alkyl- and dialkylzirconocenes in the presence of CuCl because this type of reaction had not been reported previously. The reaction of alkylzirconocenes such as $[Cp_2Zr(n\text{Bu})Cl]$ and $[Cp_2Zr(n\text{Oct})Cl]$, prepared by hydrozirconation of alkenes, with alkynes gave the carbometalated products in low yields ($< 25\,\%$). Further investigation, however, revealed interesting reactivity patterns of dialkylzirconocenes. Thus the reaction of dialkylzirconocenes such as $[Cp_2Zr(n\text{Bu})_2]$ and $[Cp_2Zr(n\text{Oct})_2]$ (**4**) with phenylacetylene in the presence of CuCl afforded, after hydrolysis, a mixture of three products. As shown in Scheme 2, **5**–**7** are obtained when **4** was used as the substrate. Despite the fact that a mixture of products was formed, this result clearly indicated that the carbometalation of nonactivated alkynes by dialkylzirconocene had taken place.

[*] Prof. Dr. T. Takahashi, Y. Liu, Dr. B. Shen, Dr. M. Kotora
Catalysis Research Center and Pharmaceutical Sciences
Hokkaido University
Kita-ku, Sapporo 060 (Japan)
Fax: (+81) 11-706-3274
E-mail: tamotsu@cat.hokudai.ac.jp

[**] A part of this work was supported by the Grant-in-Aid for Scientific Research (no. 09440212) from the Ministry of Education, Science, Sports and Culture of Japan.

Supplementary information for this article is available on the WWW under http://www.wiley-vch.de/home/angewandte/ or from the author.

 © WILEY-VCH Verlag GmbH, D-69451 Weinheim, 1999 1433-7851/99/3807-0949 $ 17.50+.50/0